THE ASTROPHYSICAL JOURNAL, 217:186–196, 1977 October 1

THE SPECTROSCOPIC ORBIT AND MASSES OF SK 160/SMC X-1*

J. B. HUTCHINGS AND D. CRAMPTON†
Herzberg Institute of Astrophysics
A. P. COWLEY*
University of Michigan
AND
PATRICK S. OSMER
Cerro Tololo Inter-American Observatory
Received 1977 February 16; accepted 1977 March 30

ABSTRACT

Thirty-one spectrographic observations have been obtained of SK 160, with dispersions from 12 to 52 Å mm^{-1}. Radial velocities from these lead to a spectroscopic orbit which implies masses of 16.2 ± 1.4 $M_\odot$ and 1.02 ± 0.20 $M_\odot$ for the two components, and $i = 64°$–$70°$ for the system. Mass exchange appears to be by Roche lobe overflow rather than a strong stellar wind. There are also spectroscopic indications of a heating effect by X-rays, but no line velocity distortions are found, in rough agreement with calculations. Radial velocities and intensity measurements of He II λ4686 emission suggest that the line is formed in a hot spot between the two stars and slightly trailing the X-ray source.

Subject headings: stars: eclipsing binaries — X-rays: binaries

I. INTRODUCTION

The SMC X-1/SK 160 system is of particular interest among the X-ray sources because it is both an eclipsing and pulsating X-ray binary, making determination of the individual masses and primary radius possible. Further, because it is in the Small Magellanic Cloud, its distance, and hence absolute magnitude, are known quite well. The binary period of the system has been estimated as $3^d.89217$ by Tuohy and Rapley (1975) and recently revised (van Paradijs 1977) to 3.89238 days, and Primini and Rappaport (1977) have derived orbital parameters of the X-ray star from analysis of the arrival times of the X-ray pulses which have a period of $0^s.71$. These authors show that the orbit is circular, $e \leq 0.0016$, and that the projected orbital velocity of the X-ray star, K_x, is 301.5 ± 4 km s^{-1}. A previous attempt (Osmer and Hiltner 1974) to derive a spectroscopic orbit for SK 160 yielded a velocity curve with very large scatter and hence a poorly determined value for the orbital velocity amplitude of SK 160 (K_0, ~25 ± 8 km s^{-1}). Combined with the X-ray data, this value of K_0 and a preferred value of 40 km s^{-1} lead to estimates of the mass of the X-ray source, presumably a neutron star, in the wide range $1.1 < M_x < 4.0\ M_\odot$ (Primini *et al.* 1976). We have obtained a series of spectra of SK 160 with improved resolution in order to set firmer limits on the masses of both components.

* DAO Contribution No. 330 = NRC No. 15612.

† Guest Observers, Cerro Tololo Inter-American Observatory, supported by the National Science Foundation under contract No. NSF-C866.

II. OBSERVATIONS

Most of the observations were obtained with the RC spectrograph and Carnegie image tube on the CTIO 4 m telescope. The spectra were well widened (1.0 or 2.0 mm), and recorded on baked III-aJ plates. The largest part of our observations were obtained with a grating giving 26 Å mm^{-1} in the wavelength region 3900–4900 Å. Spectra were also obtained at other dispersions, in different wavelength regions, and a few with the 1.5 m spectrograph attached to the RC focus of the 4 m telescope. These latter observations were taken on IIa-O baked plates without an image tube. A journal of all observations is given in Table 1.

III. SK 160

The spectrum of SK 160 is that of an early B supergiant, with some unusual features. The equivalent width of Hγ (~1.6 Å) is typical of early B class Ia stars (Balona and Crampton 1974). Comparison with HD 91943 (B0.7 Ia), and HD 91969 (B0 Ia), both having normal CNO abundances according to Walborn (1976), indicates a spectral type ~B0 but with abnormally weak Si IV, O II, and C III lines. However, the spectrum is very similar to those of two other SMC members, SK 82 and SK 103, recently described by Walborn (1977) as being deficient in metals compared to galactic supergiant stars of normal abundance. The spectrum appears to be slightly variable, being earliest (~B0) between phases 0.15 and 0.5 and latest (~B0.5) around phase 0.9. Some of the lines, particularly the helium singlets, apparently vary in

TABLE 1

SK 160 OBSERVATIONS

Plate	Dispersion (Å mm^{-1})	Region	HJD (2,443,000+)	Phase*	Radial Velocities (km s^{-1}) Abs (wt)	4686 em	Ca II K
177.....	26	Blue	50.607	0.958	172 (3)	...	...
178.....	26	Blue	50.671	0.976	173 (2)	...	...
179.....	26	Blue	50.732	0.991	169 (3)	171 (3)	...
180.....	26	Blue	50.799	0.008	217 (0)	...	...
181.....	26	Blue	50.848	0.021	...	160 (2)	...
182.....	26	Blue	50.885	0.031	184 (2)	...	...
186.....	26	Blue	51.741	0.250	202 (2)	−54 (2)	...
187.....	26	Blue	51.786	0.262	211 (3)	−98 (3)	...
190.....	40†	Blue	52.717	0.501	168 (3)	164 (3)	80
191.....	40†	Blue	52.836	0.532	167 (3)	188 (3)	122
192.....	40†	Blue	53.589	0.725	170 (2)	298 (2)	151
193.....	40†	Blue	53.726	0.760	172 (3)	380 (2)	153
194.....	40†	Blue	53.840	0.790	171 (2)	427 (2)	...
204.....	12	Blue	63.655	0.311	194 (3)	...	...
213.....	12	Blue	66.515	0.046	182 (2)	...	...
218.....	12	4700	66.834	0.128	209 (4)	28 (4)	...
220a....	26	Blue	67.522	0.305	194 (4)	−25 (4)	...
b....	26	Blue	67.567	0.317	201 (4)	−33 (4)	...
221.....	52	Red	67.613	0.328	204 (2)	...	...
222.....	26	Blue	67.667	0.342	195 (5)	−145 (5)	64
223.....	26	Blue	67.718	0.355	...	...	...
225.....	26	Blue	67.846	0.388	180 (3)	−48 (3)	...
226.....	26	Blue	69.625	0.845	163 (5)	406 (3)	...
227.....	52	Red	69.673	0.858	155 (2)	...	...
228.....	26	Blue	69.727	0.871	162 (5)	333 (5)	122
229.....	26	Blue	69.819	0.895	177 (4)	388 (4)	...
251.....	47	Blue	113.603	0.144	207 (2)	−86 (2)	...
252.....	47	Blue	113.628	0.151	199 (2)	−98 (2)	...
257.....	47	Blue	114.577	0.395	173 (2)	−97 (2)	...
263.....	47	Blue	115.546	0.644	166 (2)	−220 (2)	...
268.....	47	Blue	116.538	0.898	183 (2)	400 (2)	...

* Phase defined by $T_0 = 2{,}443{,}066.335 + 3.89217\,E$.

† Spectra taken with 1.5 m spectrograph.

intensity in an erratic way. The C III, O II absorption blend near 4650 Å appears to vary systematically in intensity, virtually disappearing when He II λ4686 is strong, indicating that variable weak emission is filling in the absorption. Tracings of the spectra substantiate this.

IV. RADIAL VELOCITY MEASUREMENTS

Most of the measurements were made on the DAO oscilloscope display machine ARCTURUS. Typically, about five Balmer lines, five He I lines, and five other lines, principally of He II, Si IV, and N III, were measured. Standard star spectra were measured in the same way. Excellent agreement was found between different measures of the same plate, the agreement between mean values for the same plate being typically within 7 km s^{-1}.

Two corrections which appear to be instrumental were applied to the velocities. A small hour-angle dependence was found in the standard star velocities and the velocity residuals from the orbital determination. Corrections of $\sim$10 km s^{-1} were indicated at large hour angles ($\gtrsim$4 hours), and were applied to the velocities from four spectra. A correction of +10 km s^{-1} was required to bring the five velocities of SK 160 and the standard taken at 47 Å mm^{-1} into agreement with the other velocities. These corrections did not affect the values of the orbital parameters deduced from the data, except to reduce the scatter.

As noted below, individual line velocities from the same plate agree well with each other with the exception of the velocities from the He I λ4387 line. The velocities from this line and others which occasionally differed by more than 2 σ from the mean because of flaws or blends or noise, were rejected. After this rejection, the average internal error of the mean plate velocity is $\pm$6 km s^{-1}. The external error or the error determined from the agreement of velocities from different spectra of a constant velocity star is usually about 50% larger than the internal error, or $\sim$9 km s^{-1} in this case.

The He II λ4686 emission line was seen on almost all spectra, although its intensity varies considerably with phase, as was noted by Osmer and Hiltner. The profile also is phase dependent, apparently being divided by one or more absorptions at some phases. The profile was measured as a single broad feature and also as individual peaks.

Calcium II K absorption was measured when present, although blending with other features creates difficulties. On the red plates, Hα appears as a broad emission.

The velocities are given in Table 1.

V. RADIAL VELOCITIES FOR ORBITAL DETERMINATION

We are concerned that we use velocities which represent most reliably the orbital motion of the primary star. No line asymmetries were noted in the spectrum of SK 160 (apart from the expected blends), but the measured velocities were carefully scrutinized with the following points in mind:

1. *Stellar wind.*—Hot supergiants generally have a stellar wind, whose strength is primarily a function of luminosity and temperature. Stars at the position of SK 160 in the H-R diagram generally do not show strong evidence of mass loss; but there are exceptions, and binaries may have enhanced mass loss due to additional tidal effects. The signatures of a weak stellar wind are P Cygni profiles at Hα and Hβ, a velocity-excitation correlation, and a Balmer velocity progression (see Hutchings 1976 for a full discussion). *None of these effects is present in SK 160.* All measured lines give the same velocity within the expected uncertainty at all phases. This is in contrast to the other X-ray binaries with supergiant primaries: Cyg X-1, Vela X-1, and 3U 1700−37. Of these, Cyg X-1 shows the least evidence for a stellar wind, and its spectrum is most similar to SK 160. This, and the other arguments given below, suggest that SK 160 is intrinsically less luminous than the other known supergiant primaries of X-ray binaries. This and the high X-ray luminosity may be the reason why the X-ray heating is more pronounced in this system.

2. *Lines with systematic differences.*—The image tube velocities from the He I λ4387 line showed a large scatter and a mean velocity 18 km s^{-1} more positive than that of other lines. None of the other lines either individually or grouped according to ions showed any velocity differences from each other or the mean.

3. *Velocity differences from cycle to cycle.*—Osmer and Hiltner reported that the velocity curve may not repeat from cycle to cycle. Our observations, taken over parts of 17 cycles, suggest that the velocity curve is stable. Furthermore, the systemic velocity which we observed is similar to that observed by Osmer and Hiltner. Hence, we find no systematic differences suggesting that non–phase-related velocities occur.

These considerations led to the adoption of the mean velocities in Table 1 for orbital determination. The velocity of plate 180, a weak exposure, was $\sim$40 km s^{-1} above the mean of the four plates taken before and after it on the same night, and hence it was rejected. The remaining velocities were weighted on a scale of 1 to 5 by consideration of the plate quality, dispersion, and internal errors of the mean velocities.

To enable the reader to judge some of these conclusions, we show in Table 2 individual line velocities from two subsets of the spectrographic data. The table shows the principal lines measured, their individual scatter, and systematic differences between lines and plates. Lines were weighted empirically from these figures, as shown, in deriving the adopted plate velocities.

VI. RADIAL VELOCITY DISTORTIONS

Before interpreting the radial velocities in terms of orbital motion, we considered possible distortions caused by the proximity of the components and the large X-ray flux from one of them. Calculations of this type have been reported by Hutchings (1973), Wilson and Sofia (1976), Milgrom (1977), van Paradijs (1977), and Moulding (1977). Of the above, only Milgrom (1976) applied his calculations specifically to Balmer lines in SMC X-1, allowing for the X-ray heating and stellar distortion and gravity darkening in the line from the primary star. Van Paradijs shows that the latter effects may be important in some lines in HD 77581. We therefore made specific calculations of lines of O II, He I, Si IV, and H for a grid of models, with and without X-ray heating, to apply to SK 160. These calculations and results are reported in full elsewhere (Hutchings 1977). The result in brief is that the most likely SK 160 model ($R \sim R_{\rm crit}$, $T_{\rm eff} \sim$ 31,500 K, heated to reproduce the optical light curve), shows that distortions expected in all these velocities are small, and fairly sensitive to $T_{\rm eff}$. This should allow a good check on $T_{\rm eff}$, if the simple model applies. In practice we do not see a distortion from a simple sine curve of any of the predicted types, all of which are necessarily symmetrical about phases 0.0 and 0.5. Thus, either the model is essentially correct and distortions are small, or there are other effects present (disk, hot spot, stream?) not included in the model. Either way, we do not have sufficient information to allow for these effects in our observations and must simply take the velocities as representing the stellar velocity. The formal error derived by fitting the observations with a sine curve is $\sim$8 km s^{-1}, similar to the error we estimated for the velocities. However, it is obvious that they *do* deviate systematically from a simple sine curve, as can be seen by the numbers in Table 3, and from Figure 1. We can think of no simple disk or stream model which will give a distortion of this nature, nor do we find that consideration of eclipse of the primary by an opaque region near the secondary will explain it.

We therefore present the velocities in Table 1 without correction, and note that our results may eventually be modified by use of a model that does reproduce the $O - C$ variations shown. We note specifically that the distortions of the type calculated by Milgrom for heating effects only in the Balmer lines are not present, and that distortions of the type calculated by van Paradijs, particularly for Si IV, are not seen either.

Rappaport (private communication) reports that SMC X-1 was off during 2,443,067.5–68.0, and on at normal intensity during 2,443,068–70. Our observations over these dates show no systematic differences between on and off states. The phase coverage (Table 1) is small, but we must further conclude that we find no positive evidence for X-ray heating in radial velocities or line intensities. On the other hand, we note that HZ Her shows optical heating effects during its X-ray OFF phases.

TABLE 2

SOME INDIVIDUAL LINE VELOCITIES FROM SK 160 SPECTRA (in km s^{-1})

		Balmer						He I					N III	Si IV	Si III	He II			He I	Wtd
Plate	Phase	Hβ	Hγ	Hδ	Hε	H8	H9	4713	4471	4387	4143	4036	4097	4088	4552	4541	4200	Mean	Mean	Mean
218.....	0.13	223	...	...	...	...	...	232	266:	...	...	...	...	...	208	...	...	228	230	231 ± 7
220.....	0.30	196	232	...	...	...	...	227	212	263	171	203	185	204	...	231	232	214	215	210 ± 6
204.....	0.31	...	216	230	204	...	...	...	...	...	192	...	...	194	...	...	170	201	192:	205 ± 7
220.....	0.32	...	190	191	...	...	...	...	204	220	181	199	203	190	...	...	196	197	201	194 ± 2
222.....	0.34	...	195	225	...	...	...	...	210	198	239	177	...	206	...	...	...	207	206	206 ± 5
225.....	0.39	...	187	193	...	...	...	210	219	225	...	213	...	...	197	...	...	206	217	203 ± 5
226.....	0.85	165	179	174	...	...	...	...	157	202	231	160	...	...	181	204	...	184	174	177 ± 6
228.....	0.87	...	178	164	...	...	...	196	153	160	194	176	190	159	175	160	203	174	176	174 ± 4
229.....	0.90	...	207	217	201	...	...	184	185	237	169	199	171	200	...	210	...	200	199	198 ± 4
Line weights.....		1	2	2	1			1	2	0	1	2	1	2	1	1	1			
Line means.....		195	198	199	202			210	196	215	197	190	187	192	190	210	200			
Plate means*.....		209	198	196	200			204	201	197	197	197	196	199	198	193	197			
Mean deviation.....		−14	2	3	2			6	−5	18	0	−7	−9	−7	−8	8	3			
190.....	0.50	...	...	184	...	178	...	206	...	...	211	150	...	204	...	...	...	172	176	178 ± 9
191.....	0.53	...	161	172	174	192	189	178	170	177	...	165	...	...	...	...	...	178	173	177 ± 5
192.....	0.72	...	151	210	159	156	172	178	169	...	192	192	...	172	...	...	...	176	178	175 ± 5
193.....	0.76	...	...	204	173	166	175	...	190	171	...	202	...	153	...	...	...	181	188	180 ± 6
194.....	0.79	...	212	...	154	216:	199	...	189	124	...	131	...	167	...	...	...	173	148	181 ± 12
Line weights.....			2	1	1	2	2	1	2	0	1	2		2						
Line means.....			175	193	165	178	184	192	182	160	(211)	168		174						
Plate means*.....			176	177	177	176	177	175	177	177	(172)	176		176						
Mean deviation.....		−1	16	−12	2	7	7	17	5	−17	(39)	−9		−2						

* Unweighted mean of plate means for spectra in which line is measured.

TABLE 3

SMC X-1 ORBITAL SOLUTIONS

K (km s^{-1})	V_0 (km s^{-1})	e	ω (radians)	$\Delta\phi$*	P (days)
			Absorption		
25 ± 3.....	181 ± 1	0.36 ± 0.09	6.2 ± 0.2	~0.01	(3.89217)
21 ± 3.....	180 ± 2	(0)	(0)	−0.04	(3.89217)
†19 ± 2.....	180 ± 2	(0)	(0)	(0)	(3.89217)
19 ± 2.....	180 ± 2	(0)	(0)	(0)	3.86 ± 0.03
			He II 4686		
244 ± 16.....	143 ± 13	0.10 ± 0.07	1.3 ± 0.8	0.54 ± 0.01	(3.89217)
†245 ± 16.....	150 ± 12	(0)	(0)	0.53 ± 0.012	(3.89217)
254 ± 18.....	155 ± 14	(0)	(0)	(0)	(3.89217)
247 ± 5.....	150 ± 4	(0)	(0)	0.52 ± 0.003	3.899 ± 0.003

* Phase shift from X-ray minimum.

† Adopted (see text).

VII. ORBITAL SOLUTION AND MASSES

In Table 3 we show some formal orbital solutions. The X-ray orbit constrains us to use $e = 0$ and defines T_0, so we are obliged to adopt the parameters that fit most of the three sets. We have fixed P at the well-defined X-ray eclipse value, but find that the optical observations yield a best fit value which does not differ from this, nor give significantly altered parameters.

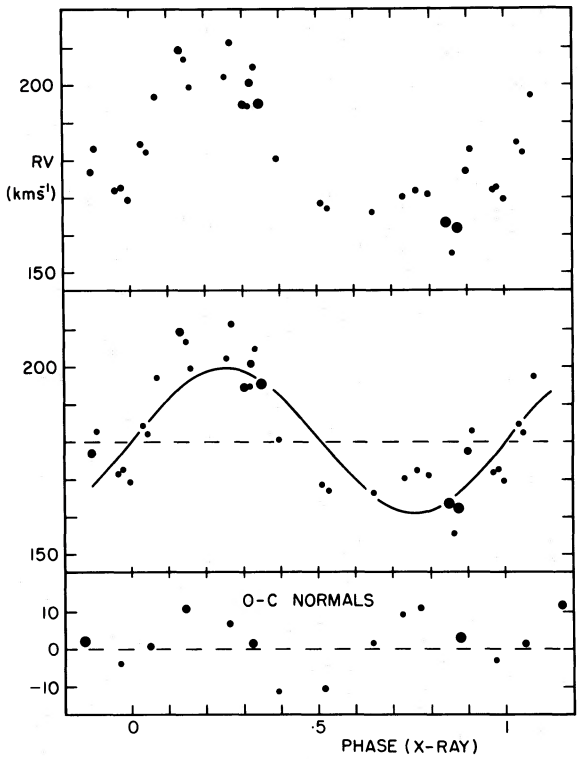

FIG. 1.—SK 160 absorption line velocities. Sizes of points indicate weight. Center panel shows adopted orbital solution, with $e = 0$ and T_0 fixed by X-ray data. Systematic $O - C$ trends shown in lower panel.

It is worth noting that the apparently well-defined eccentric orbit is spurious, and this is a warning that similar results for other supergiant X-ray binaries may also be. The fit with T_0 a free parameter is only slightly better, indicating a phase shift of ~0.04 away from the X-ray value. We can see no physical reason for believing this, and therefore reject it.

The adopted orbit has a low value of K, yielding a mass ratio (q) of 15.9 and mass function of 0.00277. Table 4 shows the full range of possible numbers and masses. A number of discussions (e.g., Primini *et al.* 1976; Whelan and Wickramasinghe 1976; Hutchings 1975*a*; Petro 1976) show that $i \leq 70°$ is probable from analysis of the light curve and eclipse duration.

If the Roche lobe is exactly filled, the eclipse duration of ±28° gives $i = 65°$ for $q = 15.9$, and masses of 17.3 and 1.09 $M_\odot$. If the Roche lobe is underfilled by 10%, these values correspond to $i = 70°$. Since rotation seems to be synchronous (see below), Roche geometry seems a good assumption and we suggest that i lies in the range 64°–70°. We note that the luminous nature of the primary may affect the geometry of the Roche surfaces (Kondo, McCluskey, and Gulden 1976) in the sense of preferring a model which slightly underfills the Roche lobe. We therefore see that the masses are well determined: $M_x = 1.02 \pm 0.20\ M_\odot$ and $M_o = 16.2 \pm 1.4\ M_\odot$, given that our velocity curve does represent the primary star motion. The pulsar mass is slightly lower than previously considered for this system but is certainly within accepted values for a neutron star, and is not in conflict with any of the above referenced papers. The primary mass is certainly low for a B0 supergiant, by a factor of about 2 (see below). It appears that SMC X-1, 3U 1700−37, Vela X-1, and Cen X-3 all have undermassive primaries, which must have lost a large amount of mass in their prior histories. We should therefore expect that Cyg X-1 has a similarly undermassive primary. (This would imply $M_o \sim 15$

TABLE 4

SMC X-1 COMPONENT MASSES IN $M_\odot$

K (km s^{-1})	q (M_o/M_x)	$f(m)$ ($M_\odot$)	$i = 64°$		$i = 70°$		$i = 90°$	
			M_o	M_x	M_o	M_x	M_o	M_x
17.....	17.7	0.00199	17.0	0.96	14.8	0.84	12.3	0.70
19.....	15.9	0.00277	17.3	1.09	15.1	0.95	12.6	0.79
21.....	14.4	0.00374	17.6	1.22	15.4	1.07	12.8	0.89

$M_\odot$ and $M_x \sim 10\ M_\odot$ for that system, thus still not eliminating the black hole problem.) It is also interesting to note that none of the primaries show abundance anomalies (apart from SK 160 being normally metal weak for the SMC), as does, e.g., HD 163181, which is undermassive by a factor of ~ 3 or more (Hutchings 1975*b*).

The primary star radius is found to be 14 (polar)–18 (substellar) $R_\odot$, if it nearly fills its Roche lobe, and this yields a $\log g = 3.25 \pm 0.13$. This radius for a B0 star implies a bolometric luminosity of $\sim 5 \times 10^{38}$ ergs s^{-1}, which is about the same as the X-ray flux, *if* it is isotropic. The low mass of the secondary then would have to exceed its Eddington limiting luminosity at times. However, it has been argued (e.g., Milgrom 1976) that there may be blanketing in the orbital plane, which may (or may not) alleviate this problem. We discuss the primary luminosity later.

a) He II *4686 Velocities*

The He II 4686 line appears as a broad weak (but variable) emission moving approximately in antiphase with respect to the supergiant absorption lines. The He II λ4686 emission velocities yield the orbital elements shown in Table 3. The large velocity amplitude indicates that the emission is not associated with either of the stars, and so the phase shift of 0.54 phase is acceptable and of interest. The small formal errors on this phase shift suggest that it is real. The naive interpretation is that the emission arises from a region off-axis, trailing the X-ray star, about midway between the X-ray star and the surface of the primary. The small apparent eccentricity is very unlikely to be real, in view of the measuring errors and the small space available for an orbit to be eccentric. The $e > 0$ parameters do not indicate a significantly better or different fit to the observations.

In several cases the emission is double and velocities were derived for each peak, as well as the emission taken as a whole, with a central dip. These are shown in Figure 2. Interpretation of the emission as one broad line occasionally overlain by absorption yields a smooth curve, suggesting that this is a valid interpretation. The amplitude of the velocity variation suggests that the line is formed between the stars. A double-peaked structure might arise in a ring surrounding the compact object, but should have the velocity amplitude of that object, which is 301.5 km s^{-1}—larger than our observed amplitude.

We also considered whether the observed velocity amplitude and phase could arise partly from orbital motion in a ring around the secondary. However, the orbital velocity implied by the phase shift (~ 75 km s^{-1}) placed the region ~ 0.2 of the binary separation away from the secondary, which in turn implied a K lower than the observed value. This possibility therefore seems to be eliminated.

The λ4686 emission is discussed further below.

VIII. SPECTROPHOTOMETRY

Rectified intensity tracings were made of all spectrograms of sufficient quality, as marked in Table 1. Intensity calibrations were obtained for spectra 204 onward: mean calibrations for the emulsion and color were used for the others. Plots were generated for all spectra with 1, 1.5, and 2.5 Å smoothing windows, and Table 5 lists the principal measurements made. Some of the measured quantities are shown in Figure 3, and averaged tracings of features of interest are shown in Figure 4.

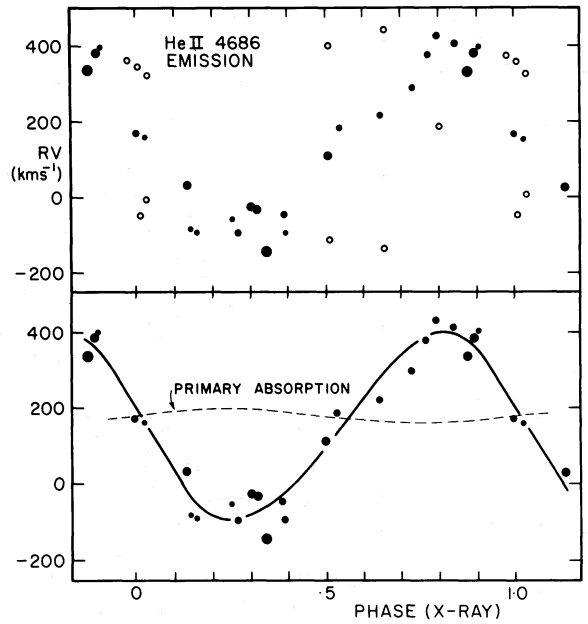

FIG. 2.—He I 4686 velocities. *Solid points*, emission as a single broad feature. Sizes of point indicate weight. *Open points*, individual peak velocities where line is double. Lower panel shows best fit curve.

TABLE 5

SMC X-1 SPECTROPHOTOMETRIC MEASUREMENTS

Phase (X-ray)	Plate	Balmer Lines				He I								He II				Si IV 4089	Si III 4552	Mg II 4481	O II 4351	N III, C III ~4640 (EM)
		Hδ		Hγ	Hβ	4026		4387		4471		7 lines		4541		4686 (EM)						
		D	D	EW	D	D	F	D	F	D	F	ΣD	$\bar{F}$	D	P	F	EW	D	D	D	D	P
0.030....	182	28	33	1.62	18	17	4.0	12	3.6	26	3.4	97	3.7	...	4	7.5	0.3	14	7	4	10	4:
0.128....	218	...	...	...	25	...	...	...	...	17	5.0	...	...	Wk	17	7.0	1.7	...	Wk	≤3	...	6
0.145....	251	22	21	1.44	16	14:	5.5	10	4.6	11	6.5	60	5.4	6	25	6	1.3	8	4	4:	5	3:
0.151....	252	23	21	1.48	12	15	5.3	13	4	17	5	77	4.8	6	18	7	1.3	9	≤3	5	7	...
0.262....	187	26	28	2.10	...	14	5.3	12	4.7	19	5.0	77	5.0	...	15	3	0.6:	6	6	5	10	...
0.305....	220	...	22	1.31	15	...	...	10	...	17	4.6	73:	4.6:	5	12	8	1.1:	...	≤4	4	5	...
0.317....	220	27	22	1.37	15	19	4.9	12	4.8	17	4.5	77	4.8	5:	10	8.5	1.0	11	5:	3	4	5:
0.342....	222	22	23	1.55	9	14	4.9	15	4.2	18	4.4	83:	4.5	7	9:	10	0.8:	9	5	6	7	≤5
0.388....	225	23	22	1.65	10	8	7.5	14	4.7	12	5.3	64	5.9	7	7	10	0.7	8	5	5	7	5:
0.501....	190	30	34:	1.9:	...	25	4.4	...	...	...	...	92:	4.4:	11	10:	10	1.0	8	≤4	...	...	...
0.644....	263	25	21	1.64	35:	16	6.5	9	5	13	6	73	5.9	7	12	12	1.4	10	≤2	≤2	≤5	...
0.725....	192	20	21	1.05	...	15	4	14	3.6	21	4.3	81	3.9	≤8	14	7.5	1.0	10	...	≤3	7	...
0.760....	193	22	23	1.14	...	20	3	11	3	18	4.7	83	3.4	...	13	7	0.8	12	...	6	6	8
0.845....	226	30	33	1.9	10	11	4.2	17	3.9	22	4.6	99	4.2	≤5	15	11	1.7	11	10	≤3	6	5:
0.871....	228	23	27	1.42	8:	13	3.5	14	4.0	22	4.0	89	3.8	≤3	13	9	1.3	9	8	4	5	...
0.895....	229	24	25	1.50	7:	11	4.9	16	4.7	17	6.9	70	4.7	≤3	9:	10:	1.0:	9	4:	4	8	3:
0.899....	268	...	23	1.64	21	...	...	6	4.4	15	5	...	4.7:	...	12	4	0.4	...	...	5	5	2:
0.975....	178	29	28	1.7	...	...	...	14	4.2	20	5.0	...	4.6	≤3	...	...	...	12	7	5	12	...

NOTE.—D, line central depth in % of continuum. P, peak intensity in % of continuum. EW, equivalent width in Å. F, full width in Å at half-peak or central intensity. ΣD, sum of central depths of He I λλ4009, 4026, 4120, 4143, 4387, 4471, 4713. $\bar{F}$, mean of F values of He I λλ4026, 4143, 4387, 4471, 4713. Numbers of significant figures quoted reflect quality of data.

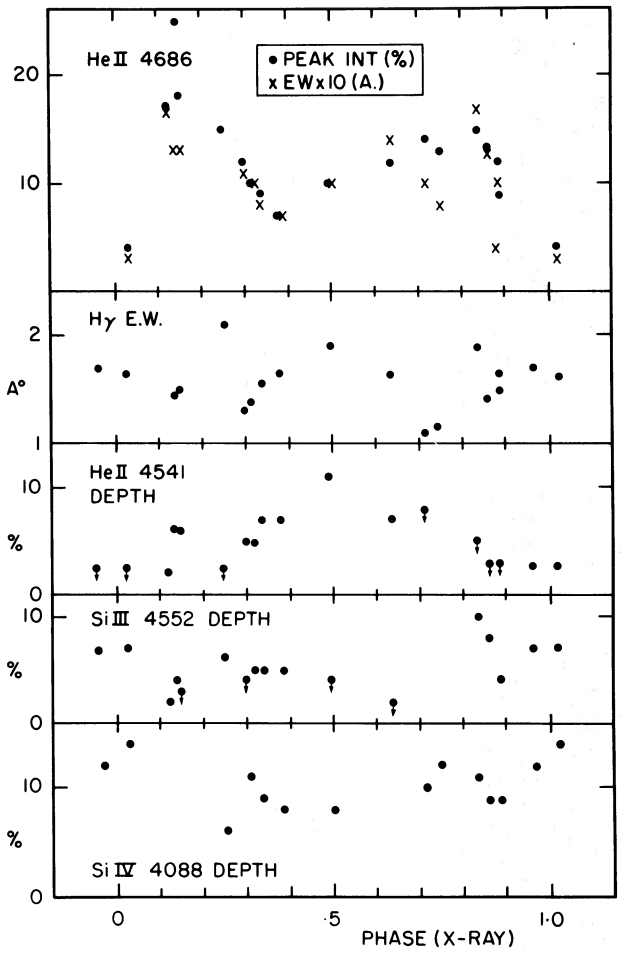

FIG. 3.—Spectrophotometric quantities which vary with orbital phase.

The most interesting feature is the He II λ4686 line. Following the radial velocity results, the line was assumed to be a single feature with occasional absorption dips, and the peak intensities and equivalent widths (EW) were measured on the assumed symmetrical broad peak. These show very similar behavior, being large at quadratures and diminishing at both conjunctions. The drop at $\phi \approx 0.5$ is interesting, as it suggests the presence of obscuring material near the X-ray source. Note that the behavior of the peak intensity is almost independent of the profile assumed. The EW, however, is not, and shows variations between that shown, and irregular with little phase dependence, depending on the assumed profile. It is clear that the line is strongest near the phase 0.25 quadrature and mostly double through phases 0.6–1.0.

In view of the heating effect indicated by the light curve, it is of interest to look for spectroscopic evidence for this. The most suitable lines in the spectrum are all weak: Mg II λ4481, Si III λ4552, He II λ4541, Si IV 4088. All of these indicate that the side of the primary facing the X-ray source is slightly hotter. There is insufficient information to look for asymmetry about the line of centers. The range in mean spectrum is of the order of 0.5 to 1 spectral subclass, which corresponds to a change of $\sim$1000 K (Morton and Adams 1968). This is roughly what the light curve suggests. Surface gravity changes might be seen in Balmer or Si IV lines. The former do show a large variation ($\pm$25%) with no clear phase dependence. There is some suggestion that they are weaker at quadratures, both in depth and EW, but the meaning of such a change is not clear. Silicon IV is strongest near phase 0, which may be due to the low g unheated back side of the primary. Nitrogen III varies similarly. He I is marginally stronger in phase 0.8–1.0. For most lines the data are noisy but consistent with a primary star tidally distorted and heated by the X-ray companion (see Hutchings 1977).

Finally, the mean EW of Hγ is 1.55 Å, which corresponds to $M_v = -6.6$. Extreme values give a range in M_v of -5.9 to -7.5. A distance modulus of 19.0 (Gascoigne 1974; van den Bergh 1976) and a mean absorption of 0.3 for the Small Magellanic Cloud (SMC) gives $M_v = -6.1$ for SK 160 for a mean $M_v = 13.2$. These numbers place SK 160 in the mass range 30–40 $M_\odot$ on the H-R diagram, where stellar winds are usually seen, and indicate again the undermassive nature of the star.

IX. ROTATION

The He I lines were measured for rotation, as they are strong and numerous enough to yield a good average, and are mainly rotationally broadened in this type of star. The mean FWHM for the He I lines is 314 km s^{-1}. Allowance for instrumental broadening yields a $V \sin i$ value of 200 km s^{-1}. This corresponds to synchronous rotation for a radius 0.66 of the separation. The Roche lobe for the mass ratio we have derived has polar, equatorial, and substellar radii of 0.56, 0.64, and 0.75, respectively ($V \sin i$ = 226 to 193), which are therefore satisfactorily close to the mean value above. This rotation reduces log g from 3.2 to 3.1 (25% in g) at the equator for the radius we have derived and so is a small perturbation on the tidal distortion.

The λ4686 mean profile has a FWHM of 550 km s^{-1}, which must be close to $V \sin i$ if the line is rotationally broadened. This would be the orbital velocity about the secondary at a distance of $\sim$0.03 of the separation (S) of the star. Since the velocity amplitudes suggest that the λ4686 emission is found at a distance 0.17S, it seems unlikely that the line is rotationally broadened. If it is thermally broadened, a temperature of $\sim 2 \times 10^7$ K is required.

X. THE SYSTEMIC VELOCITY

The value of V_0 for the absorption lines (180 km s^{-1}) is reasonable for the SMC, whose mean value from Feast, Thackeray, and Wesselink (1961) is 166 km s^{-1} with a standard deviation of 16 km s^{-1}.

The V_0 value for λ4686 emission is lower than for the absorption. There is no clear explanation. This

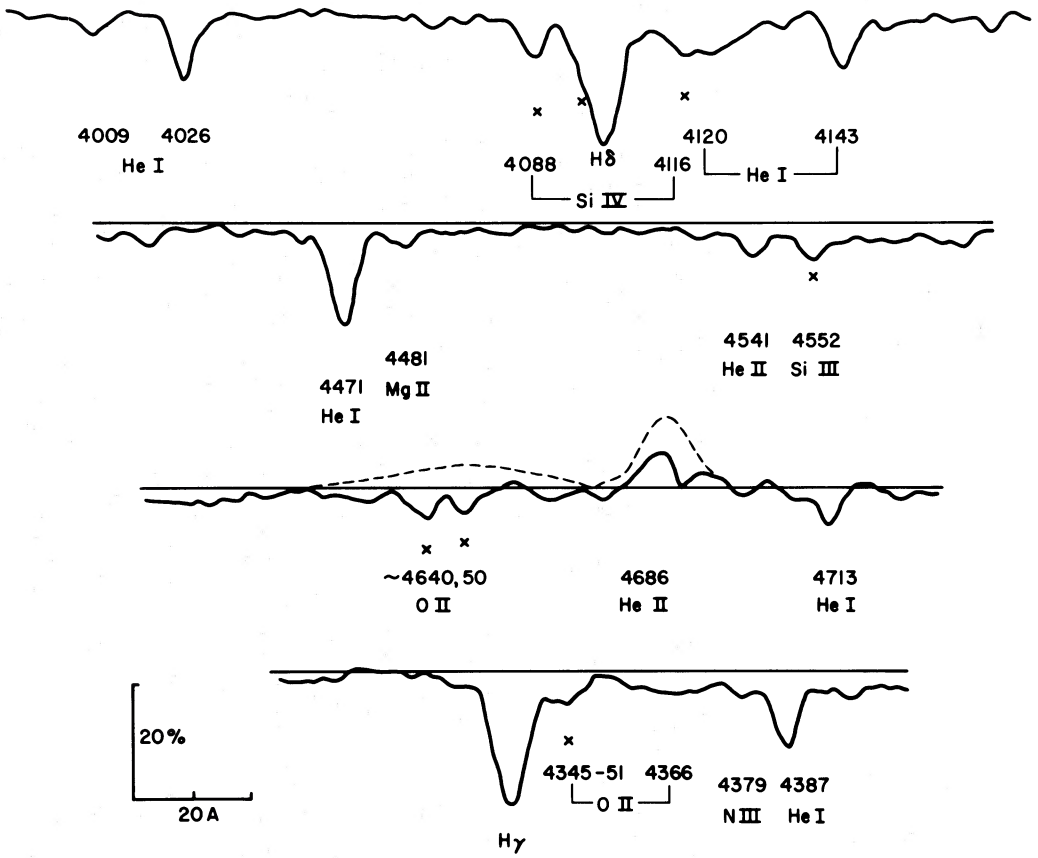

FIG. 4.—Tracings of SK 160 spectra (26 Å mm^{-1} data) averaged over all phases, smoothed over 2 Å. Normal line depths of O II, Si IV, N III in galactic supergiants shown by symbol ×. Dotted line represents mean emission profile of λλ4634–4660 blend and λ4686.

line is often found to be *redshifted* with respect to other lines in W-R stars. It is possible that part or all of the velocity curve of λ4686 is blue-shifted by the presence of a redward absorption (by a stream or general infall), but there is no indication in the profiles that this is so.

XI. THE Hα LINE AND RED SPECTRUM

Two spectrograms were obtained of the red region, at phases near the two quadratures. Hα has a broad single-peaked emission profile, on each, with velocities which follow the primary star within the errors of measurement, and definitely dissociate it from the secondary or the λ4686 region. The line has a half-width of ~750 km s^{-1}, which is broader than any other line in the spectrum, absorption or emission. Clearly, greater phase coverage is needed to study the behavior of this unique feature. At present we speculate that it arises in an extended region surrounding the whole system and may be broadened by mass motions. The peak emission is ~12% above the continuum, and EW is ~2.2 Å. On the ~0.85 phase spectrum there is a redshifted absorption, whose velocity is ~ +300 km s^{-1}. This could originate in a gas stream of the Roche lobe overflow, if seen in projection against a continuum from the secondary.

Otherwise, the spectrum appears normal in this region. Helium I absorption is seen with normal velocity at λ5015, 5875, 6678. Carbon III λ5696 is probably present, and the diffuse interstellar band at λ6284 is seen.

XII. THE Ca II K LINE

On several plates a line was measured at the Ca II K position (see Table 1). Unfortunately the coverage is poor as the spectrum is weak and near the edge of the plate in most cases. The most reliable data are from the IIa-O plates, and there is a marginal suggestion of a phase dependence. If this is real, it suggests a variation antiphased with respect to the primary. The V_0 value is 80 km s^{-1} and may be affected by interstellar absorption. If so, the amplitude is also unreliable. As it stands then, we surmise that there may be a Ca II K line formed with $K \geq 60$ km s^{-1} on the same side of the center of mass as the X-ray source.

The best spectra in this region show the presence of a sharp component, interstellar in appearance, and a

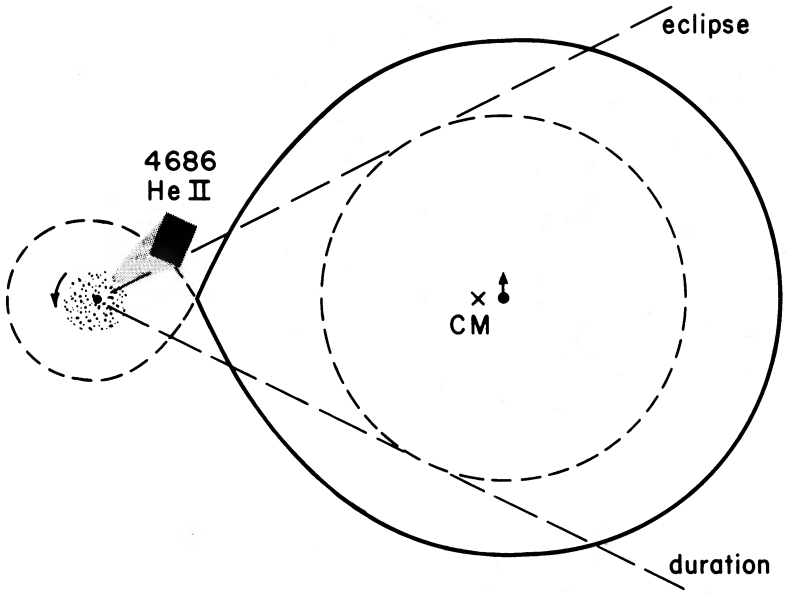

FIG. 5.—Projection in orbital plane of SMC X-1 model for $q \approx 16$. He II 4686 emission from dark area if motion is purely orbital; light area is included if motion is partly circulation about secondary. Some emission probably originates from entire secondary Roche lobe. Dashed straight lines show lines of sight at edges of eclipse at $i \approx 65°$.

broader line. Since there may be both galactic and SMC interstellar absorption and stellar Ca II and He I λ3926, it is obvious that we need better observations to clear up this point.

XIII. DISCUSSION AND SUMMARY

In Figure 5 we show our proposed model for the system. The primary spectrum shows evidence for heating by X-rays, in agreement with the light curve. There is no evidence for a stellar wind. Stellar rotation is close to synchronous for a star filling the Roche lobe of the mass ratio found. The implied inclination (64°–70°) of the system agrees with that found by light curve analysis. There is λ4686 emission which is probably off axis, between the stars, which is partially occulted at both conjunctions. We think this is a hot spot where a stream from Roche lobe overflow (or mass flow from the heated, distorted side of the primary, if the Roche lobe is slightly underfilled) intersects a disk about the secondary. The width of the line does not show much change with phase if we interpret it in this way, but it is a little narrower near X-ray eclipse. It is much weaker but not absent during eclipse, so that it must be formed in a region which lies or extends above the orbital plane by about 0.25 of the separation of the star centers, if it is all localized as the velocity curve suggests. It is strongest at ~0.15 phase and has a secondary maximum of ~0.85 phase, with a drop through ~0.4 phase. This suggests the presence of an opaque disk around the secondary and hence a low-velocity mass transfer (Roche lobe overflow?), rather than a stellar wind model—and the off-axis location of the λ4686 emission. This in turn suggests that the observed X-radiation is higher than that in the orbital plane, which may explain the absence of a larger heating effect on line velocities or in the light curve. Note that Avni and Milgrom (1977) and van Paradijs and Zuiderwijk (1977) conclude from light curve analyses that there is a luminous disk about the secondary.

Primini *et al.* (1976) found a discrepancy between observed and calculated absolute bolometric magnitudes. If we assume a mean $T_{\rm eff}$ of 31,500 K (including the heating effect), $R = 17\ R_\odot$ and a bolometric correction of 3.0 mag, we find $M_v = -5.8$, which is somewhat less than the observed value of −6.1. This is smaller than the discrepancy found by Primini *et al.* because we have used a higher temperature, and may be attributable to uncertainty in the SMC distance modulus. Otherwise, we have to adjust $T_{\rm eff}$ to 34,000 K or R_x to 19.5 $R_\odot$, both of which are outside reasonable limits. We suggest that extra luminosity may come in some way from degeneration of X-rays, or that the flux distribution in the primary is not normal if it has lost much of its initial mass. There is no direct evidence for either of these possibilities.

It is also not clear where the broad Hα emission line originates, and further study of this feature may reveal more details of the mass flow in the system. It is also possible that a study of the Ca II K line would be valuable in this way. Although we have significantly improved our knowledge of the velocity curve, further observations to study the velocity distortion are clearly desirable.

REFERENCES

Avni, V., and Milgrom, M. 1977, *Ap. J.* (*Letters*), **212**, L17.
Balona, L. A., and Crampton, D. 1974, *M.N.R.A.S.*, **166**, 203.
Feast, M. W., Thackeray, A. D., and Wesselink, A. J. 1961, *M.N.R.A.S.*, **122**, 433.
Gascoigne, S. C. B. 1974, *M.N.R.A.S.*, **166**, 25p.
Hutchings, J. B. 1973, *Ap. J.*, **180**, 501.
———. 1975*a*, *Ap. J.*, **201**, 413.
———. 1975*b*, *Pub. A.S.P.*, **87**, 245.
———. 1976, *Ap. J.*, **203**, 438.
———. 1977, *Ap. J.*, in press.
Kondo, Y., McCluskey, G. E., and Gulden, S. L. 1976, NASA SP-389, p. 499.
Milgrom, M. 1977, *Astr. Ap.*, **54**, 725.
Morton, D. C., and Adams, T. F. 1968, *Ap. J.*, **151**, 611.
Moulding, M. 1977, *Astr. Ap.* (in press).
Osmer, P. S., and Hiltner, W. A. 1974, *Ap. J.* (*Letters*), **188**, L5.
Petro, L. 1976, thesis, University of Michigan.
Primini, F., and Rappaport, S. 1977, preprint.
Primini, F., Rappaport, S., Joss, P. C., Clark, G. W., Lewin, W., Li, F., Mayer, W., and McClintock, J. 1976, *Ap. J.* (*Letters*), **210**, L71.
Tuohy, I. R., and Rapley, C. G. 1975, *Ap. J.* (*Letters*), **198**, L69.
van den Bergh, S. 1976, *IAU Colloquium No. 37* (Dordrecht: Reidel).
van Paradijs, J. A. 1977, preprint.
van Paradijs, J., Takens, R., and Zuiderwijk, E. 1977, *Astr. Ap.* (in press).
van Paradijs, J. A., and Zuiderwijk, E. 1977, preprint.
Walborn, N. R. 1976, *Ap. J.*, **205**, 419.
———. 1977, *Ap. J.*, **215**, 53.
Whelan, J. A. J., and Wickramasinghe, D. T. 1976, *M.N.R.A.S.*, **174**, 29.
Wilson, R. E., and Sofia, S. 1976, *Ap. J.*, **203**, 182.

A. P. Cowley: Department of Astronomy, University of Michigan, Ann Arbor, MI 48109

D. Crampton and J. B. Hutchings: Dominion Astrophysical Observatory, 5071 W. Saanich Rd., Victoria, B.C. V8X 3X3, Canada

P. Osmer: Cerro Tololo Inter-American Observatory, Casilla 63-D, La Serena, Chile